Electrode worksheet interface behaviour during resistance spot welding of Al alloy 5182

M. Rashid*[1], J. B. Medley[2] and Y. Zhou[2]

Resistance spot welding of aluminium alloy 5182 with spherical tip electrodes was investigated. Surface interaction between electrode and worksheet was focussed to understand the pitting behaviour of electrode. Both experimental work and finite element analysis were employed. It was found that the interaction between electrode tip and worksheet surface that occurred during the load 'squeezing' phase of the welding sequence of resistance spot welding process had a significant effect on the electrode pitting behaviour. At this interface, squeezing caused surface shear stress that strongly suggested the possibility of slip at the periphery of the contact region. This suggestion of slip was consistent with disrupted oxide layer and reduced electrical contact resistance near the periphery of the contact. At the beginning of the current phase, current concentrated near the periphery caused high constriction resistance which resulted in alloying, pickup and eventually pitting of electrode in a ring around the contact centre.

Keywords: Resistance spot welding, Aluminium alloy, Electrode pitting, Surface interaction, Oxide layer, Contact resistance

Introduction

Demand for light weight vehicles encourages auto industry to use light metals such as aluminium and magnesium for auto body frames and structures. Aluminium alloys with their high strength/weight ratio and corrosion resistance property are preferred choice for better fuel economy and environment.[1,2] Aluminium alloy 5182, for its good formability and low cost final surface preparation, is very popular in the automotive industry.[1,3] Since it is fast, requiring no skilled labour and easily automated, resistance spot welding (RSW) remains the main joining process for most automotive sheet metal applications.[2,4] The electrical, mechanical and thermal properties of aluminium alloys make RSW more difficult and have been facing two major problems: short electrode tip life and inconsistent weld quality particularly joint strength and nugget size.[5,6]

Short electrode tip life for RSW of aluminium alloys is due to the aggressive electrode degradation which occurs in three sequential steps.[7,8] It starts with alloying between electrode and worksheet material. If the alloyed phase sticks with the electrode, it is known as pickup; pickup disturbs the load and current distribution which exaggerate the alloying process locally. However, if the alloyed phase adheres to the worksheet surface, this result in a pit created at the electrode tip and is generally known as electrode pitting. For a given welding condition, electrode pitting is the most detrimental factor to weld quality and gradually deteriorate the joint strength during continuous RSW process.[7–9]

Aluminium (worksheet) and copper (electrode) have relatively low bulk resistivity and therefore, the main source of heat during RSW of aluminium alloys is the contact resistance at the interfaces.[10,11] This 'contact' resistance influences the weld strength and electrode tip life and depends heavily on the tribological features of the contact.[7,8] The most significant tribological features of aluminium sheet surface have been reported as oxide layer (composition, thickness and uniformity), roughness of the surface and presence of an added chemical compound or lubricant. While surface roughness may have some influence at low loads, most contacts at the electrode–worksheet interface (E/W) become fully plastic during the weld sequence and thus the roughness is mostly crushed. Oxide layer, on the other hand, may be the main factor in the generation of electrical contact resistance at the interfaces. The presence of a chemical or lubricant could also alter the electrode life[6,8,12] and one of the recent studies[8] suggests that a suitable lubricant can influence electrical contact resistance by modifying the oxide layer.

In practice, the oxide layer on aluminium sheet is not uniform in its geometry or composition.[3,13,14] The oxide layer on AA5182 is particularly complex with other oxides and hydro oxides often present.[3] The cracking and/or removal of this oxide layer are considered to be very important as the current flow through the interfaces is mainly possible through the cracks that permit metal to metal contacts.[10,13] The electrical contact resistance at the sheet to sheet interface or faying surface (FS) provides the main source of heating for the weld nugget formation and thus some resistance is necessary. However, the electrical contact resistance at the E/W

[1]CANMET-MTL, Natural Resourced Canada, Ottawa, ON, K1A 0G1, Canada
[2]CAMJ, Dept. of Mechanical and Mechatronics Engineer, University of Waterloo, ON, N2L 3G1, Canada

*Corresponding author, murashid@nrcan.gc.ca

© 2009 Institute of Materials, Minerals and Mining
Published by Maney on behalf of the Institute
Received 7 October 2008; accepted 22 December 2008
DOI 10.1179/136217109X406947

interface is generally unwanted and believed to be the main reason of short electrode tip life.[6,10–12,15] The current concentration at the metal to metal contacts causes high local heat generation which in turn starts local melting and alloying and hence pitting of electrode. Although, it is well established that oxide layer cracking during the squeeze phase is essential for RSW of aluminium alloys, the knowledge is very limited regarding the location of this oxide layer cracking and its relationship to the electrode degradation pattern.

Load is also considered to be an important factor in determining the nature of the contact at the interfaces.[10,15,16] However, for aluminium alloys, the contact pressure alone is not enough to disturb the surface oxide layer and sliding between surface is more effective.[15] At the E/W interface, this could be quite effective in reducing the electrical contact resistance.[10]

Finite element analysis (FEA) of RSW has been a popular investigative tool. Because of the loading sequence and weld schedule, this process is generally considered and modeled as an incrementally coupled mechanical–electrical–thermal process.[17–20] In general, most of the FEA models use flat tip electrodes and thus avoid having to include a Hertzian type contact at the E/W interface. However, for spherical tipped electrodes which are often used for RSW of aluminium alloys, the contact area changes continuously during the processes[18] and it is very important to include this behaviour in the modeling. Owing to mechanical, thermal and electrical properties of aluminium alloys, the electrode indentation into the worksheet and sheet separation at the peripheral regions of the FS become more severe than for steel and the possibility of slip at the E/W interface becomes more likely.

The purpose of the present study is to investigate the influence of surface interaction at the E/W interface on the electrode pitting behaviour during RSW of AA5182. The behaviour of the oxide layer at this interface is of particular importance. Since interfacial slip could influence the oxide layer, an attempt is made to measure it. Both experimental investigations, including a detailed study of electrode pitting to explore its link with contact behaviour and FEA are conducted. In particular, the initiation of electrode pitting is examined along with its location on the electrode tip.

Materials and methods

Aluminium alloy (AA5182) with a thickness of 1·5 mm was used as worksheet material throughout the present study, the composition of which is Al–4·71Mg–0·32Mn–0·19Fe–0·08Si–0·05Cu–0·01Cr–0·01Zn–0·02Ti (wt-%). The sheet surface was mill finished and without any chemical or further physical treatment. The electrodes used for these experiments were class I type made from copper and 0·15% zirconium.[21] These electrodes were truncated (taper angel 60°) with a spherical tip having a 10 mm face diameter and a 50 mm radius of curvature (Fig. 1). All welding was performed using a 170 kVA pedestal type medium frequency direct current spot welder (Centerline Limited, Windsor, Canada). Unless otherwise mentioned, all RSW was performed using parameters (Table 1) that had been selected based on a series of preliminary investigations of RSW with this alloy.

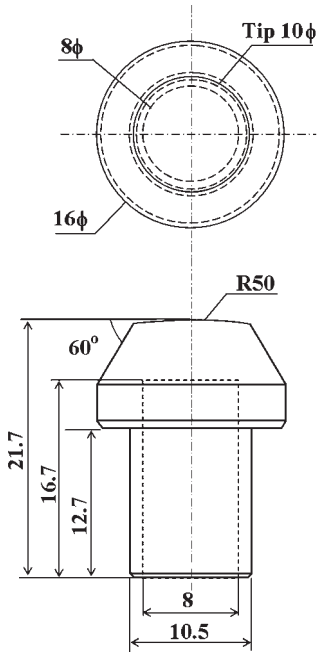

1 Electrode configuration (mm) for RSW

The first step of electrode pitting, i.e. melting of worksheet surface or alloying between electrode and worksheet surface starts as early as within the first few spot welds. Even evidence of worksheet surface melting after first spot weld of AA5182 is available.[7] However, the electrode pitting process during the very early stage is not significant and difficult to trace. Electrode pitting process gradually increases and early work for AA5182 with similar welding condition showed signs of electrode pitting between 25 and 50 spot welds which became clearly visible after 50–60 spot welds.[7,8,22] For the present work, since the shape of the electrode pitting was the main subject, electrode pitting between 50 and 100 spot welds during continuous RSW process was presented to demonstrate a clear pitting behaviour of electrode during the early stages of electrode life. Furthermore, during a continuous spot welding process, it is almost impossible to take out the electrode cap for analysis and replaced them back in the same position for further welding. For this reason there are several other techniques that indicate the gradual progress of electrode pitting.[5,7,8,13,23] The presence of electrode material on the worksheet surface is considered as a strong evidence of electrode pitting process.[5,7,13] A carbon imprint of the electrode tip is another method that represents the general morphology of the tip surface including the electrode pitting and contact diameter. Carbon imprints collected at regular intervals during continuous spot welding process are the most common

Table 1 Welding parameters and weld schedule (1 cycle=16·67 ms)

Welding parameters	
Force	6 kN
Current magnitude	29 kA
Weld rate	20 spots per minute
Squeeze time	25 cycles
Current time	5 cycles
Hold time	12 cycles

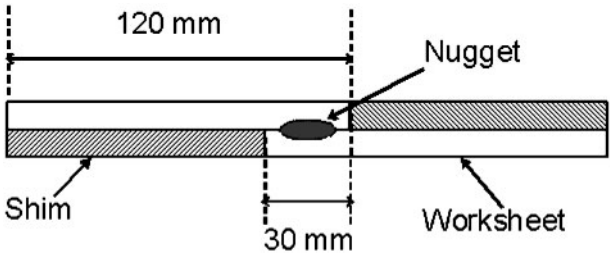

2 Geometry of overlapped test specimen

methods to show the gradual progress of electrode pitting process.[5,7,8] These two methods alone or in combination are the most common methods to present electrode pitting progress during continuous RSW process. For the present work, since continuous welding was performed, both the presence of electrode material on the worksheet and carbon imprints were used to present electrode pitting behaviour during the early stage of electrode life.

Electrode pitting experiments

These experiments were performed to observe the electrode pitting behaviour in the range of 50–100 spot welds for the as received surface of AA5182. RSW was performed using the welding parameters listed in Table 1. Standard coupons of 50×400 mm aluminium strips were made from the 1·5 mm thick worksheets and 10 spot welds were performed 35 mm apart along each coupon. Repeated sets (3–5) of experiments, with each set consisting of 100 spot welds (using 10 standard coupons for each set) were performed. A fresh pair of electrodes was used for each set. Carbon imprints of the top (positive) electrodes were obtained to observe the pitting behaviour.

Contact area experiments

A series of experiments were performed to explore the links between contact area size and electrode surface pitting. RSW was performed with different current times (1–5 cycles where 1 cycle=16·67 ms) on overlapped specimens (that were used for shear force measurements) of 30×120 mm with an overlap of 30 mm (Fig. 2). Using a stereomicroscope at low magnification and Image-Pro software, contact diameters were measured (Fig. 3) from the indentations (or plastic deformations) of the worksheets that were produced by the electrodes during RSW. Other than current time, all other welding parameters were kept constant at the values given in Table 1. Before any welding was done, five tests were performed on the overlapped specimens with only the squeezing part of the RSW sequence. The intent of these 'squeezing only' tests was to obtain the diameter of the electrode worksheet contact at the end of squeezing and they were each done with a fresh electrode pair to avoid the permanent contact mechanics changes that might have been present in electrode pairs with an RSW history. The subsequent welding tests involved using five additional electrode pairs and subjecting each of them to a randomised sequence of five different current times (Table 2). The welding sequence was randomised so that any progressive and permanent contact mechanics changes from previous RSW would be included in the scatter of the data.

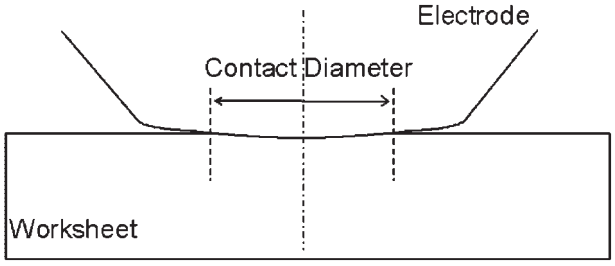

3 Schematic of measurement of contact diameter between electrode and worksheet

Effect of squeezing experiments

During contact area experiments, a difference in the topographical appearance of the central part and periphery of the contact zone was observed. Since, it was suspected that this topography could be related to the electrode pitting behaviour, a more detailed investigation of the worksheet topography after the squeezing period of RSW process was performed.

The as received worksheet surfaces were relatively smooth compared with the as received electrode tips (Fig. 4) that had visible machining marks and centre line average roughness R_a values of $1{\cdot}48 \pm 0{\cdot}04$ μm (average $\pm$STD Dev.). But these machining marks soon disappeared as successive RSW were performed. Thus, the study of the worksheet topography required more than just using the as received electrode tips. One approach would have been to use electrode tips that had been subjected to many welds (say 50–200) but these used electrodes had considerable variation in both macroscopic and microscopic surface geometry. Thus, it was decided for the sake of precision to produce polished surfaces with a closely controlled geometry and to use them in subsequent testing. Electrode tips were polished

Table 2 Randomised sequence of RSW tests involving different current times

Electrode			Current time
Pair	Test sequence	Test number	(cycles)
A	First	A.1	3
	Second	A.2	1
	Third	A.3	4
	Fourth	A.4	2
	Fifth	A.5	5
B	First	B.1	2
	Second	B.2	4
	Third	B.3	3
	Fourth	B.4	5
	Fifth	B.5	1
C	First	C.1	4
	Second	C.2	3
	Third	C.3	5
	Fourth	C.4	1
	Fifth	C.5	2
D	First	D.1	1
	Second	D.2	5
	Third	D.3	2
	Fourth	D.4	4
	Fifth	D.5	3
E	First	E.1	5
	Second	E.2	2
	Third	E.3	1
	Fourth	E.4	3
	Fifth	E.5	4

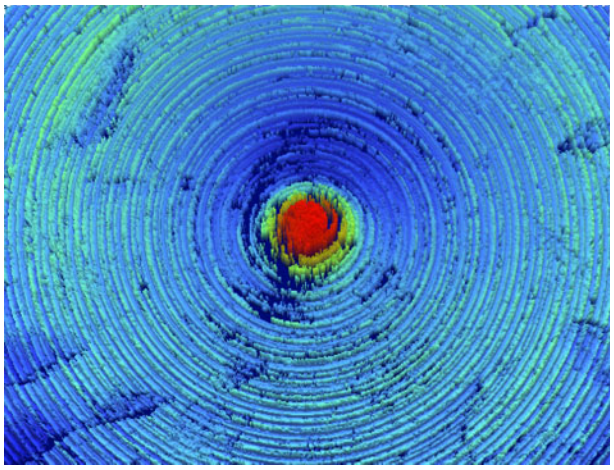

4 Tip surface of typical as received electrode showing machining marks (R_a=1·48±0·04 μm)

using abrasive paper (1200 grade silicon carbide). To accomplish this, the electrodes were rotated in a lathe and the silicon carbide paper was held manually against the electrode tips. Several electrodes (~30) were polished and radii of the tips were measured before and after the polishing using profile projector (Model PH350, Mitutoyo Mfg Co. Ltd, Japan). Only those polished electrodes that retained the as received radius of curvature (50 mm) were used in the subsequent testing (Fig. 5). The polished electrodes had a centre line average roughness R_a of 0·25±0·01 μm compared with 1·48±0·04 μm for the as received electrodes.

Squeezing only tests were performed with both the as received and polished electrodes using the overlapped specimen (Fig. 2) and same weld force of 6 kN. The intent of these new tests was to observe the effect of squeezing on the worksheet surface.

Finite element analysis

Finite element analysis of the contact mechanics during the squeeze part of the RSW schedule (before the application of the current) was performed using a commercial FEA code (ABAQUS, Hibbit, Karlsson & Sorensen Inc., Pawtucket, RI).[24] An axisymmetrical model was employed which consisted of both upper and lower electrodes and the two worksheets. This model

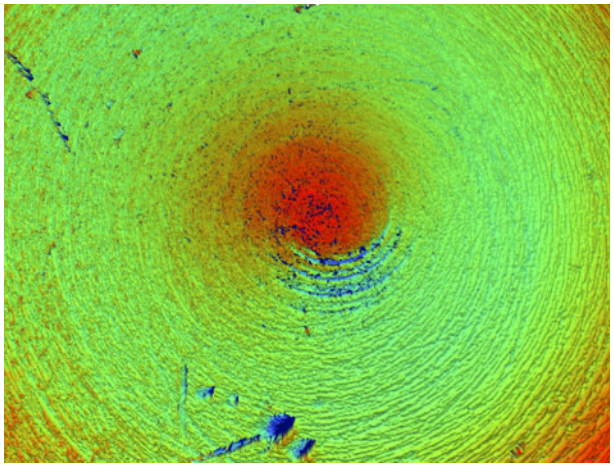

5 Tip surface of typical polished electrode (R_a= 0·25±0·01 μm) showing faint evidence of original machining marks

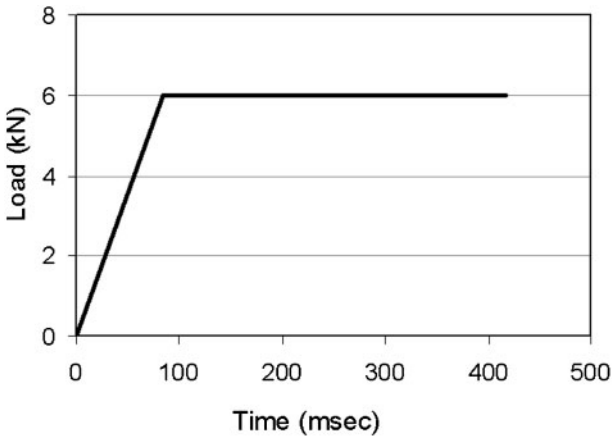

6 Loading equation of RSW setup showing load application during squeezing (note that 1 ms=0·06 cycle)

allowed the upper electrode to move down while keeping the lower electrode fixed and thus the force and boundary constraints of the actual RSW process were represented. A uniform pressure, equivalent to the weld load, was applied on the upper electrode while the lower electrode was fixed for axial (z-direction) displacement. The loading function (Fig. 6), which represented the actual loading condition observed through data monitoring system, was used as input to the FEA.

Values for yield stress, tensile stress and elongation for the worksheet material (AA5182) was obtained using standard tensile tests[25] of five specimens. Mechanical properties of the copper alloy (C15000) electrode material and remaining properties of aluminium alloy (AA5182) worksheet that were used in the FEA (Table 3) were taken from the Metals Handbook.[26] Since electrode indentation into the worksheet was extensive, an elastic-plastic model was developed using true stress and plastic strain. Four-node axisymmetric quadrilateral elements were used for both electrode and worksheet (Fig. 7). No attempt was made to model the oxide layer at the worksheet or microscopic deformation of any asperities at the surfaces.

There are three contacting interfaces in a typical RSW process: the two E/W interfaces at the top and bottom and the FS interface between the worksheets. For these interfaces, contact pair elements were used in order to permit slip at the interface and they also ensured that the surfaces in contact did not penetrate into each other during the loading.[18,24] To observe the relative motion that occurred between electrode and worksheet, a 'finite-sliding' was allowed with a coulomb friction model. The suggested range of coefficient of friction between the copper alloy electrode and the aluminium alloy worksheet had been estimated[27,28] to be in the range of

Table 3 Mechanical properties of worksheet and electrode materials[26]

Property	Worksheet (AA5182)	Electrode (C15000)
Density, kg m^{-3}	2660	8890
Yield stress, MPa	138	412
Tensile stress, MPa	276	445
Elongation, %	25	16
Young modulus, GPa	70·9	129
Poison's ratio	0·33	0·34

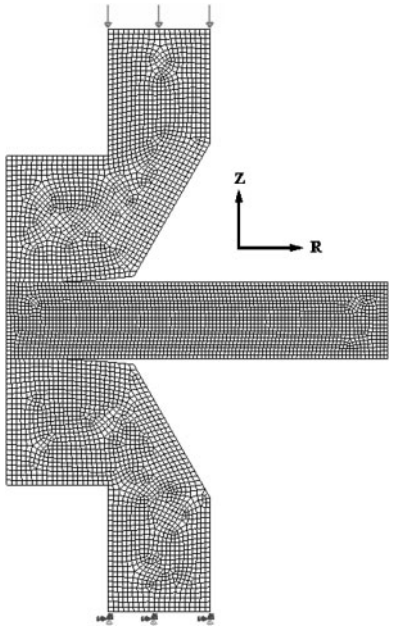

7 Axisymmetric model of RSW setup showing both electrodes and worksheets with load, boundary condition and meshing

0·3–0·6, with 0·5 as the most commonly used value. Thus, the FEA in the present study used a coefficient of friction of 0·5 between electrode and worksheet. In an attempt to ensure that the mesh was refined enough, a convergence study[24] for displacement, shear stress distribution and pressure distribution was performed. The FEA outputs include pressures, shear stresses and displacements of each surface and are presented in the 'Discussion' section of this work.

Results

Electrode pitting

From the 'Electrode pitting experiments', it was observed that after about 50–60 spot welds on the as received surface, the pitting became clearly visible on the electrode tip and some lumps of material were found on the aluminium worksheet surface. High resolution SEM of a typical contact area on the worksheet surface after 76 spot welds clearly showed these lumps (Fig. 8). Chemical analysis (energy dispersive spectroscopy) showed that these lumps had high copper content (~30 wt-%) thus indicating that these spots had Cu–Al intermetallic phases (Fig. 9). This observation clearly indicates that the alloyed material which formed between electrode and worksheet materials at the E/W interface adhered to the worksheet surface hence created a pit in the electrode surface.

One of the most important observations from these figures was the shape of these pits that formed early in the electrode life. It was observed on the worksheet surface that the transferred lumps were not located at the centre of the contact but seemed to be developing to form a ring around the centre. A similar pitting behaviour of an abraded worksheet surface was observed in another work[22] for the same material using the same procedure. This pattern of electrode pitting is designated in the present work as 'ring pitting'.

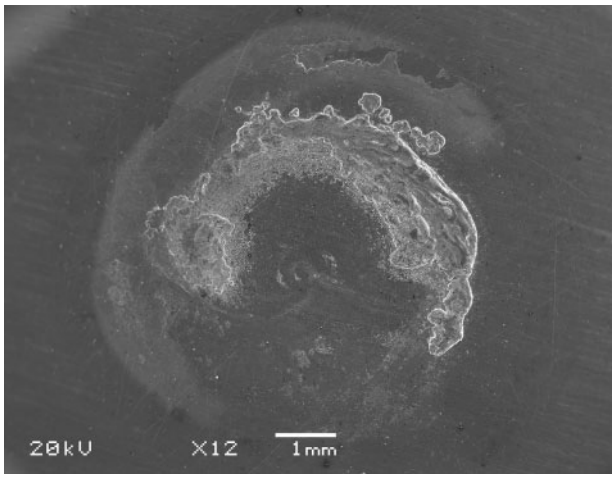

8 As received worksheet surface with alloying regions indicating electrode pitting

The next step was to investigate the location of ring pitting on the surface of electrode tip which was carried out by gathering carbon imprints of the electrode tip at the end of 100 spot welds. These imprints showed the surface topography, contact area and pitting of the electrode. It is important to mention here that all other experiments in which continuous spot welding was performed on standard coupons (including electrode life tests[7,8]) showed similar pitting behaviour and only typical examples are presented in this work. It was observed that the pitting of the electrodes which started in a ring around the centre had a diameter of ~5·0 mm (Fig. 10). Earlier, Lum[29] found similar pitting behaviour under similar welding conditions and accounted high contact resistance and hence high current density at the periphery for this pitting behaviour. However, any detail of the contact behaviour, which is the main focus of the present work, was not presented.

Contact diameter

The average contact diameters were plotted against current time (Fig. 11). The contact diameters of squeezing only test were considered to have current times of zero. The scatter in the data from the squeeze only tests was the lowest and, in retrospect, it might have been better to have a fresh electrode pair for each test involving RSW. However, the scatter in the RSW tests was not very much larger (particularly at the higher current times) and this suggested that permanent and progressive changes in contact mechanics from previous RSW were indeed quite small when 0–4 previous RSW were performed.

During the weld, the contact diameter increased with the current time. This increase in diameter was most pronounced during the first cycle as reported earlier.[30] It was observed that the contact diameter after first current cycle was $7{\cdot}65 \pm 0{\cdot}16$ mm and this was about 57% of the total change that occurred after five cycles. This change in diameter was very close to the numerical simulation results presented by Sun and Dong.[18] However, they predicted a distinct change of slope after the second current cycle whereas the present experiments showed a change in slope after the first current cycle. Interestingly, it was observed that the contact diameter at the end of squeezing was $5{\cdot}0 \pm 0{\cdot}06$ mm which was also the location of the ring pitting of electrodes. This observation

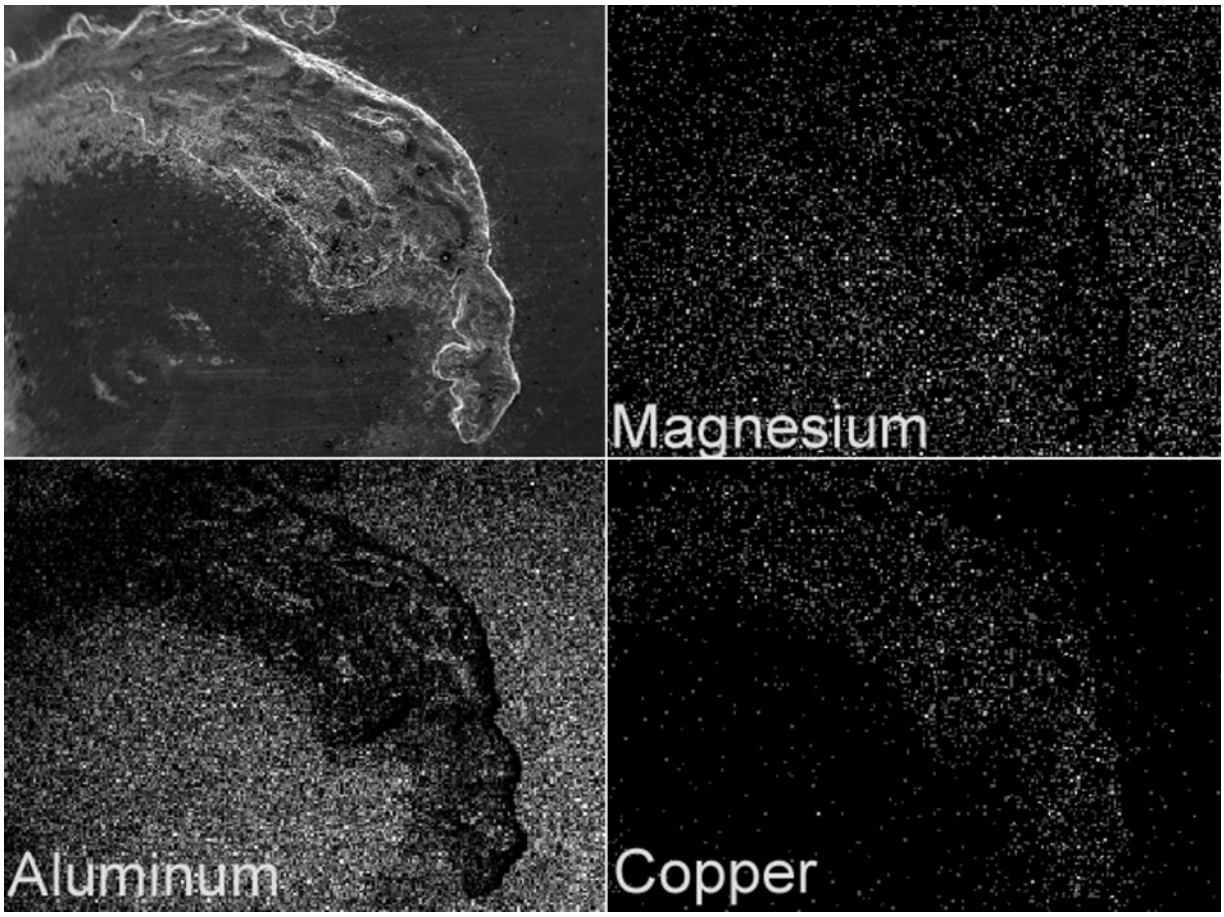

9 Energy dispersive spectroscopy analysis of alloyed spots on worksheet surface (from Fig. 8)

suggested a relationship between the ring pitting and the contact diameter before the weld current was applied.

The increase in contact diameter was almost certainly caused by the heat generation and resulting thermal softening[31] of the aluminium sheet. Owing to the high electrical contact resistance of aluminium alloys, the overall resistance at the beginning of the current time was very high but dropped sharply after about quarter of the first current cycle.[30] Thus, it was considered likely that the high heat generation in the beginning of the weld current caused a rapid initial thermal softening and hence the initial increase in contact diameter. Once the contact area started growing, both current concentration and consequently thermal softening along with contact pressure dropped[18] so that the rate of contact area growth declined.

Effect of squeezing on worksheet surface

As mentioned earlier, 'Effect of squeezing experiments' were performed specifically to investigate the effect of squeezing on the worksheet surface. In both cases (as received or polished electrodes), the contact diameters were in the range of $5{\cdot}0 \pm 0{\cdot}04$ for as-received and $5{\cdot}0 \pm 0{\cdot}07$ for polished electrodes. When in contact with the as received electrodes, the contact area on the worksheet surface revealed some aligned circular indentation marks (Fig. 12). These indentation marks were very similar in pattern to the fine machining marks

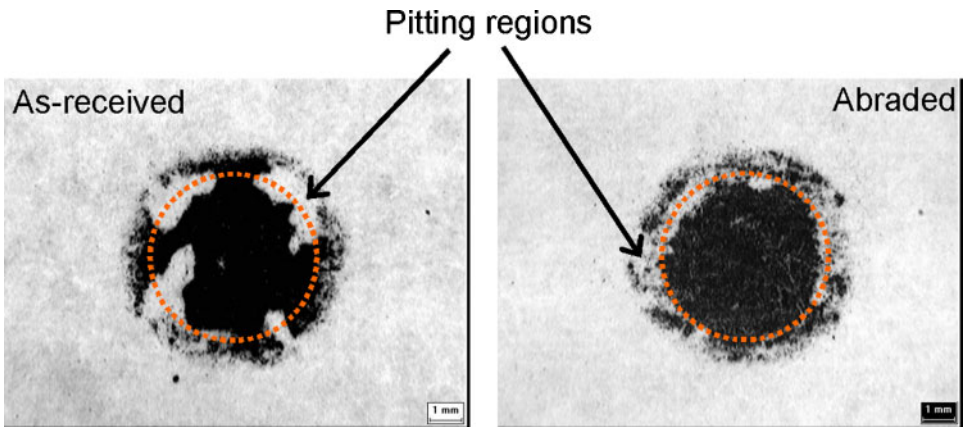

10 Carbon imprints of electrodes, ring pitting pattern during early stages of electrodes life for as received and abraded worksheet surfaces; diameter of dotted circle which link local pitted regions together is 5·0 mm

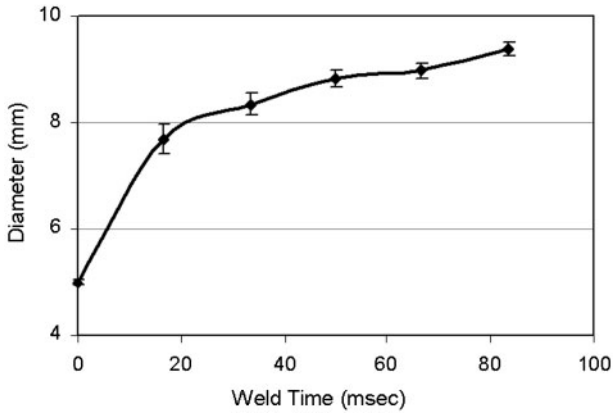

11 Contact diameter between electrode and worksheet for different weld times in milliseconds (note that 1 ms=0·06 cycle)

found on the electrode tips. However, the machining marks on the electrode tips were the same size across its face (Fig. 4) whereas the indentation marks on the worksheet surface were much more visible near the periphery than near the centre of the contact. This important observation suggested that the electrode had indented the worksheet with higher pressure at the periphery than at the centre of the contact zone.

Squeezing of the aluminium sheets with the polished electrode tips showed similar loading behaviour to squeezing with the as received electrode tips. As expected, no machining marks were observed in this case, but it was found that squeezing produced some scratches on the worksheet contact areas. These scratches were more numerous and distinct at the periphery of the contact (Fig. 13) compared with the interior zone. Furthermore, the interior contact zone appeared very similar to that of the untouched sheet surface outside of the contact.

Discussions

Shear stress and contact pressure

Finite element analysis showed that a high shear stress occurred at the periphery of the E/W contact (Figs. 14 and 15). The shear stress distribution along the E/W interface showed the highest stress values in the contact range of 4·0–5·0 mm diameter. No limit for maximum shear stress was used in the model; the maximum shear stress was found to be a little over 80 MPa near the periphery of the E/W interface. Quite interestingly, the value of the shear stress was not very significant near the centre of the contact. The contact pressure distribution along the E/W interface had similar distribution as that of shear stress, i.e. the pressure started increasing from the centre and reached maximum value near the periphery (in the range of 4·0–4·4 mm diameter) and dropped to zero at the end of the contact at 5·1 mm (Fig. 16). The contact diameter at the E/W interface obtained from this pressure distribution (5·1 mm) agreed well with the experimental value of 5·0$\pm$0·06 mm.

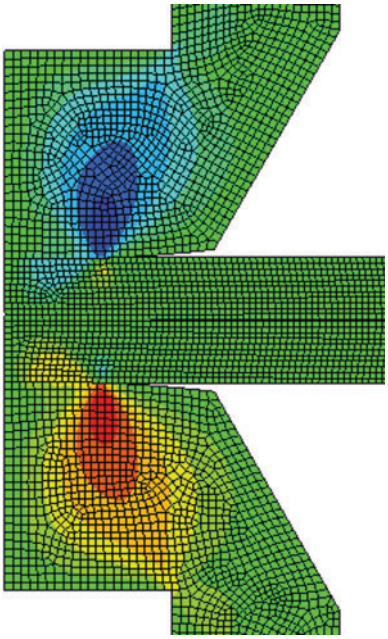

14 Shear stress distribution due to squeezing of worksheets between electrodes; contours showing shear stress distribution in entire model

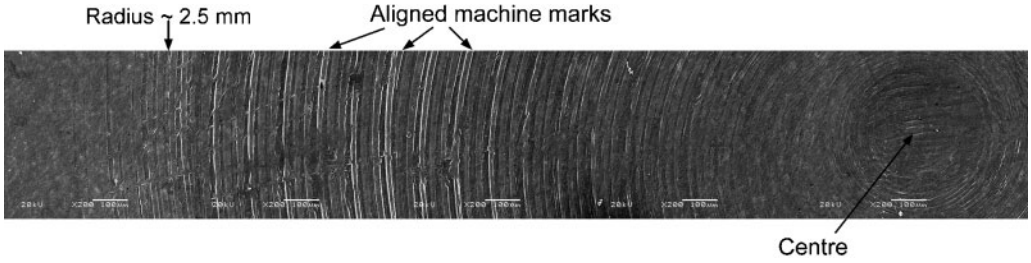

12 Effect of squeezing on worksheet surface when using as received electrode; series of SEM micrographs showing contact region of worksheet surface from periphery to centre

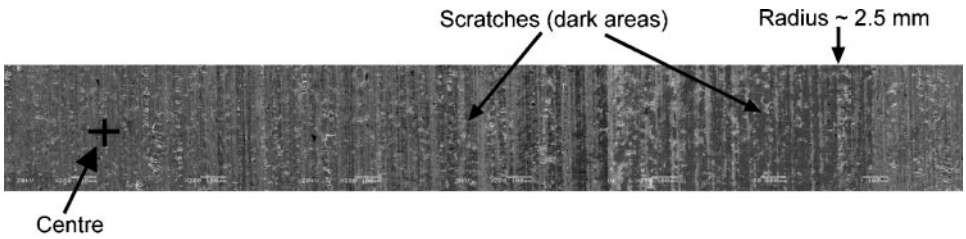

13 Effect of squeezing on worksheet surface when using polished electrode; series of SEM micrographs showing contact region of worksheet surface from periphery to centre

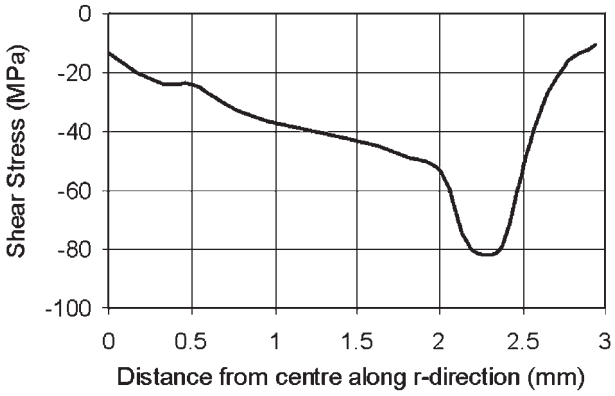

15 Shear stress distribution along E/W interface

The shear stress and contact pressure distribution developed frictional shear stress between electrode and worksheet surface. The distribution of the frictional shear stress between electrode and worksheet surface had similar behaviour, i.e. the frictional shear stress value was highest near the periphery and not very significant at the centre of the contact (Fig. 17).

Slip along E/W interface

The presence of high shear stress near the periphery could cause microscopic slip in some part of the contact region. As explained earlier, the present model characterised the tangential behaviour between electrode and worksheet surface by using the coefficient of friction of 0·5. In this case, macroscopic slip would occur at this interface if the ratio of the shear stress τ and contact pressure p becomes greater than the value of coefficient of friction μ. However, the stiffness method (penalty method) used for the formulation of this model connects the surface together with stiff spring and thus allow some relative motion (slip) between the contacting surfaces even if the shear stress to pressure ratio remain below the value of coefficient of friction.[24] The magnitude of this slip, however, is limited to the 'elastic slip', i.e. micro slip and not the macroslip or bulk sliding between contacting surfaces.

The ratio of the frictional shear stress and contact pressure was calculated and plotted as a function of radial distance from the centre along the E/W interface (Fig. 18). It was observed that the ratio of frictional shear stress and contact pressure was very low near the centre of the contact and reached the highest value at the periphery of the contact. James *et al.*[10] performed an

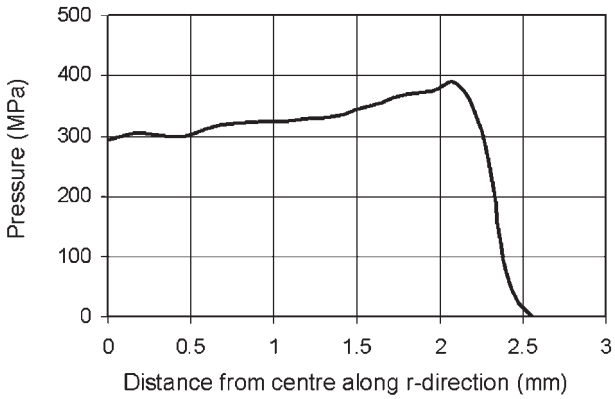

16 Contact pressure distribution at E/W interface

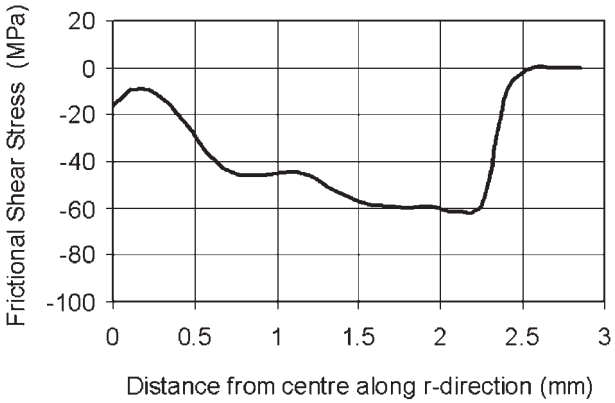

17 Frictional shear stress distribution between electrode and worksheet surfaces

FEA of the contact mechanics in RSW for 2 mm 5xxx aluminium alloy sheet using dome shaped electrode with the radius of curvature of 50·8 mm but apparently did not use contact pair (that would permit interfacial slip). They presented a somewhat similar shear stress to pressure ratio variation over the contact area and speculated that a macroscopic slip would occur near the periphery for a coefficient of friction of 0·4. However, they did not model this directly and no experimental evidence was presented.

In the present study, although, the maximum value of the frictional shear stress to pressure ratio (0·31) did not reach the value of the coefficient of friction (0·5) used for the FEA model, some micro (elastic) slip was expected to occur due to the method used for this analysis. However, it was quite interesting to observe that the shear stress to pressure ratio was relatively quite higher near the periphery than the central contact zone. Therefore, this micro (elastic) slip was expected to be higher near the periphery than the centre of the contact. The amount of this micro (elastic) slip or the relative displacement between electrode and worksheet at the E/W interface was calculated and explained as follows.

Since the electrode had spherical tip, the contact between electrode and worksheet surface started as a point and the contact area increased as the electrode squeezed in to the worksheet with increasing load. The position of a node was recorded as 'initial' position when the contact between the two surfaces was established at that node. The 'final' position of each node was obtained at the end of squeezing. The

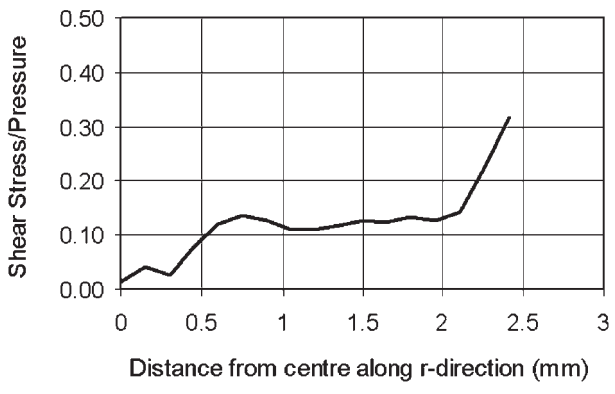

18 Shear stress as fraction of pressure at E/W interface

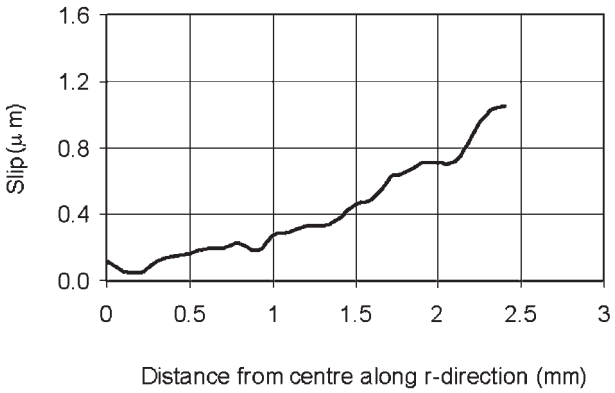

19 Amount of slip along *r*-direction between electrode and worksheet at E/W interface

difference of initial and final position provided the distance each node, while in contact with the other surface, displaced during the squeezing. These displacements for each surface were plotted along the radial direction and the difference of the two surfaces at each radius was plotted as the relative displacement or slip between the surfaces at the E/W interface (Fig. 19).

Interestingly, the amount of slip remained insignificant in the central contact zone and only started increasing from a diameter of 3·0 mm. This increase became relatively significant near the periphery; in the range of 4·0–5·0 mm. Although this slip was only elastic slip, its value was relatively much higher near the periphery than the central contact zone. This result was quite consistent with the experimental evidence where squeezing had more effect at the periphery than the centre, as shown in Figs. 12 and 13.

Although, the slip obtained using the analytical method was not as accurately presenting the slip behaviour as shown by the shear stress to pressure ratio, all these results were quite consistent in indicating that the effect of squeezing was more at the periphery than at the centre. Also, all these results were very consistent with the physical condition of the E/W interface observed experimentally. All these results and analysis clearly suggested that the squeezing process caused some micro slip only at the periphery of the contact at the E/W interface.

Ring pitting of electrode

Experimental observations and analytical model explained the 'Contact behaviour' at the E/W interface which provided the true explanation of the ring pitting of electrodes during RSW of AA5182. During squeezing, high shear stress to pressure ratio at the periphery of the E/W interface enhanced the chance of some micro slip to occur in that zone. That slip would result in significant scratching of oxide layer on the worksheet and established a good metal to metal contact zone. Although, there could be some spots in other contact zone where metal to metal contacts would established due to surface roughness (asperity tip cracking). However, the size and number of those spots would be very insignificant compare with the scratched zone near the periphery. Current always takes the least resistant path; a bigger area of metal to metal contact means less resistance. At the beginning of weld current, the periphery of the contact would provide the least resistance path for current flow from this interface. However, because of the high amount of current, there would always be constriction resistance due to current concentration. The constriction resistance near the periphery would have resulted in high heat generation in this zone. High heat generation near the periphery along with the low melting temperature of aluminium worksheet caused local melting which resulted in alloying, pickup and pitting of electrodes. A combination of all these effects led towards ring pitting of electrodes.

At the same time, due to high heat generation at this interface, the base alloy of the worksheet became soft due to thermal softening. High pressure and thermal softening of the worksheet caused electrode to penetrate into the worksheet which resulted in contact area growth between electrode and worksheet. The overall effect was reduced pressure and reduced current density hence low heat generation; the contact area growth rate decreased after first current cycle.

Conclusions

Resistance spot welding of aluminium alloy 5182 was investigated using truncated electrode with spherical tip. Surface interaction at the E/W interface was studied experimentally and with FEA. Factors influencing the pitting of the electrode tip were identified and investigated. The major findings are summarised as follows.

1. Experimental investigation as well as FEA strongly suggested that the surface interaction between electrode and worksheet during the squeezing process influenced the pitting behaviour of electrode. This conclusion was very important because much RSW research had concentrated on the complex welding process itself rather than the 'stage setting' contact mechanics.
2. The pitting of the electrode started in a ring around the centre of the electrode tip. The diameter of the initial pitting ring was in the vicinity of 5·0 mm. This diameter was the same as the contact diameter between electrode and worksheet at the end of squeezing.
3. Squeezing the worksheet surface between electrodes caused abrasion of the worksheet surface that occurred near the periphery of the contact. This abrasion was observed for both the as-received electrodes with some machining marks and polished electrodes without any apparent machining marks.
4. Results of the FEA were consistent with the experimental observations and showed significant shear stress to pressure ration near the peripheral zone of the contact than in the central zone. These results strongly suggested that, during the squeezing, some micro slip would occur in the peripheral zone in a ring whose diameter was in the range of 4·0–5·0 mm. This slip would cause enough damage to the surface oxide layer to allow good metal to metal contact between electrode and worksheet and thus a reduced electrical resistance. This, in turn, would cause current concentration and thus high heat generation due to constriction resistance and eventually ring pitting of electrode.

Acknowledgement

This study has been supported by the Natural Science and Engineering Research Council (NSERC) and the Automobile of the 21st Century (Auto21), one of the

Networks of Centre of Excellence (NCE) programs, both established by the Canadian government.

References

1. I. N. Fridlyander, V.G. Sister, O. E. Grushko, V. V. Berstenev, L. M. Sheveleva and L. A. Ivanova: *Metal Sci. Heat Treat.*, 2002, **44**, 365–370.
2. B. Irving: *Weld. J.*, 1992, 71, 44–50.
3. J. C. Kucza, J. R. Butrulle and E. Hank: 'Aluminium as rolled sheet for application-effect of surface oxide on resistance spot', Technical paper no. 970013, Warrendale, PA, SAE, 1997.
4. R. Ikeda, K. Yasuda and K. Hashiguchi: *Weld. World*, 1998, **41**, 492–498.
5. S. Fukumoto, I. Lum, E. Biro, D. R. Boomer and Y. Zhou: *Weld. J. Res.*, 2003, (Suppl.), 307s–312s.
6. E. P. Patrick and D. J. Spinella: Proc. VII Conf. on 'Sheet metal welding', Detroit, MI, USA, October 1996, AWS, paper B4.
7. I. Lum, S. Fukumoto, E. Biro, D. R. Boomer and Y. Zhou: *Metall. Mater. Trans. A*, 2004, **35A**, 217–225.
8. M. Rashid, S. Fukumoto, J. B. Medley, J. Villafuerte and Y. Zhou: *Weld. J. Res.*, 2007, (Suppl.), 62s–70s.
9. J. Peng, S. Fukumoto, L. Brown and N. Zhou: *Sci. Technol. Weld. Join.*, 2004, 9, 331–336.
10. P. S. James, H. W. Chandler, J. T. Evans, J. Wen, D. J. Browne and C. J. Newton: *Mater. Sci. Eng. A*, 1997, **A230**, 194–201.
11. A. De and M. P. Theddeus: *Sci. Technol. Weld. Join.*, 2002, **7**, 111–118.
12. P. H. Thornton, A. R. Krause and R. G. Davies: *Weld. J. Res.*, 1997, (Suppl.), 331s–341s.
13. E. P. Patrick, J. R. Auhl and T. S. Sun: 'Understanding the process mechanisms is key to reliable resistance spot welding aluminium auto body components', Technical paper no. 840291, Warrendale, PA, SAE, 1984.
14. H. Zhang and J. Senkara: 'Resistance Welding – Fundamentals and Applications', 2006, Taylor and Francis, Florida, USA.
15. E. Crinon and J. T. Evans: *Mater. Sci. Eng. A*, 1998, **A242**, 121–128.
16. H. T. Sun, X. M. Lai, Y. S. Zhang and J. Shen: *Sci. Technol. Weld. Join.*, 2007, **12**, 718–724.
17. B. H. Chang, Y. Zhou, I. Lum and D. Du: *Sci. Technol. Weld. Join.*, 2005, **10**, 61–66.
18. X. Sun and P. Dong: *Weld. J. Res.*, 2000, (Suppl.), 215s–221s.
19. J. Khan, L. Xu and Y. J. Chao: *Sci. Technol. Weld. Join.*, 1999, **4**, 201–207.
20. X. Long and S. K. Khanna: *Sci. Technol. Weld. Join.*, 2005, **10**, 88–94.
21. D. Giroux and F. D. James: 'Resistance welding manual', 4th edn; 2003, Philadelphia, PA, RWMA.
22. M. Rashid, J. B. Medley and Y. Zhou: Proc. CSME Forum 2006, Calgary, Alberta, Canada, May 2006, CSME, TB4-Paper-4.
23. D. Bracun, J. Diaci, I. Polajnar and J. Mozina: *Sci. Technol. Weld. Join.*, 2002, **7**, 294–298.
24. ABAQUS User's Manual-Interactive Version 6.5, Habbitt, Karlsson & Sorensen, Inc., USA, 2004.
25. 'Standard test methods for tension testing of materials', E8M-04, ASTM, Philadelphia, PA, USA, 2004.
26. 'Metals handbook: volume 2: properties and selection: nonferrous alloys and special purpose materials', 10th edn; 1990, Materials Park, OH, ASM International.
27. 'Metals handbook: volume 18: friction, lubrication and wear technology', 10th edn; 1990, Materials Park, OH, ASM International.
28. L. Tam, J. Hua and S. Ma: 'The Physics Factbook^{TM}', available at: http://hypertextbook.com/facts/2005/aluminium.shtml, 2005.
29. I. Lum: 'MASc thesis', 2002, University of Waterloo, Canada.
30. M. C. Thornton, C. J. Newton, B. F. P. Keay, P. S. Sheasby and J. T. Evans: Interfinish'96 World Congress, Birmingham, England, September 1996, International Convention Centre, 259–276.
31. R. Tewari, G. K. Dey, P. K. Fotedar, T. R. G. Kutty and N. Prabhua: *Metall. Mater. Trans. A*, 2004, **35A**, 189–204.